First-principles studies of electronic, optical, and mechanical properties of γ-$Bi_2Sn_2O_7$*

Chao-Hao Hu(胡朝浩)[1,2,†], Xue-Hui Yin(殷学辉)[1,2], Dian-Hui Wang(王殿辉)[3], Yan Zhong(钟燕)[1,2], Huai-Ying Zhou(周怀营)[1,2], and Guang-Hui Rao(饶光辉)[1,2]

[1] *Guangxi Key Laboratory of Information Materials, Guilin University of Electronic Technology, Guilin* 541004, *China*
[2] *School of Materials Science and Engineering, Guilin University of Electronic Technology, Guilin* 541004, *China*
[3] *School of Materials Science and Engineering, Central South University, Changsha* 410083, *China*

(Received 13 January 2016; revised manuscript received 26 February 2016; published online 20 April 2016)

The detailed theoretical studies of electronic, optical, and mechanical properties of γ-$Bi_2Sn_2O_7$ are carried out by using first-principle density functional theory calculations. Our calculated results indicate that γ-$Bi_2Sn_2O_7$ is the p-type semiconductor with an indirect band gap of about 2.72 eV. The flat electronic bands close to the valence band maximum are mainly composed of Bi-6s and O-2p states and play a key role in determining the electrical properties of γ-$Bi_2Sn_2O_7$. The calculated complex dielectric function and macroscopic optical constants including refractive index, extinction coefficient, absorption coefficients, reflectivity, and electron energy-loss function show that γ-$Bi_2Sn_2O_7$ is an excellent light absorbing material. The analysis on mechanical properties shows that γ-$Bi_2Sn_2O_7$ is mechanically stable and highly isotropic.

Keywords: γ-$Bi_2Sn_2O_7$, electronic structure, optical properties, first-principle calculations

PACS: 78.20.–e, 62.20.–x, 71.20.–b **DOI:** 10.1088/1674-1056/25/6/067801

1. Introduction

Metal oxides with the pyrochlore structure and adopting a general formula $A_2B_2O_7$ have received considerable attention due to their wide technological applications in catalysis,[1] gas sensors,[2] frustrated magnetism,[3] and superconductivity.[4] As one of the pyrochlore-type oxides, bismuth pyrostannate ($Bi_2Sn_2O_7$) has been widely studied as one of the versatile and technologically important semiconducting materials with a wide band gap. $Bi_2Sn_2O_7$ was first reported by Roth[5] and lately characterized by Brisse and Knop.[6] Previous experimental investigations have confirmed that $Bi_2Sn_2O_7$ has three polymorphs. At room temperature, $Bi_2Sn_2O_7$ probably adopts a monoclinic structure and is designated as the α phase.[7] At intermediate temperature higher than 90 °C, a cubic acentric phase (β phase) is found. At temperature above 680 °C, $Bi_2Sn_2O_7$ is the ideal pyrochlore structure with cubic symmetry and designated as the γ phase.[8]

Being similar to other Bi-containing compounds like $BiFeO_3$,[9] Bi_2WO_6,[10] and $BiVO_4$,[11] the photocatalytic property of $Bi_2Sn_2O_7$ has also been investigated extensively, owing to its potential application in the splitting of water or degradation of organic pollutants under visible light irradiation.[12–14] Wu *et al.*[12] prepared the nanocrystalline γ-$Bi_2Sn_2O_7$ by a hydrothermal route and evaluated the photocatalytic activity by the degradation of methyl orange. Tian *et al.*[13] reported the synthesis of $Bi_2Sn_2O_7$ and visible-light photocatalytic performance in the oxidation of As(III). Xu *et al.*[14] studied the fabrication and photocatalytic activity of BiOI/$Bi_2Sn_2O_7$ heteronanostructure. On the theoretical side, Walsh and Watson[15] calculated the electronic structures of both α- and γ-$Bi_2Sn_2O_7$ and highlighted the importance of covalent interactions between the electronic states of the metal with O-2p in $Bi_2Sn_2O_7$. Very recently, Fan *et al.*[16] investigated the electronic structures of $Bi_{2-x}Y_xSn_2O_7$ solid solution by performing density functional theory (DFT) calculations. In the present work, we devote great effort to investigating the optical and mechanical properties of γ-$Bi_2Sn_2O_7$ besides its electronic structure by using the first-principles DFT calculations in order to provide some helpful guidelines for the subsequent experimental work.

2. Computational details

All DFT calculations are performed by the projector augmented wave (PAW) method[17] as implemented in the Vienna ab-initio simulation package (VASP).[18,19] The exchange-correlation energy is treated within the generalized gradient approximation, using the functional of Perdew, Burk, and Ernzerhof.[20] The plane-wave energy cutoff is set to be 400 eV. A k-point spacing of about $2\pi \times 0.03$ Å^{-1} is used to generate the Monkhorst-Pack grid[21] in the Brillouin zone sampling. The fully relaxed optimization is carried out until the changes in total energy and the force on each atom are less than 10^{-5} eV and 10^{-3} eV/Å, respectively.

*Project supported by the National Basic Research Program of China (Grant No. 2014CB643703), the National Natural Science Foundation of China (Grant Nos. 11164005, 11464008, and 51401060), the Natural Science Foundation of Guangxi Zhuang Autonomous Region, China (Grant Nos. 2014GXNSFGA118001 and 2012GXNSFGA060002), and the Fund from Guangxi Provincial Key Laboratory of Information Materials of Guangxi Zhuang Autonomous Region, China (Grant Nos. 1210908-215-Z and 131022-Z).

†Corresponding author. E-mail: chaohao.hu@guet.edu.cn

© 2016 Chinese Physical Society and IOP Publishing Ltd

For optical properties calculations, a sufficient dense k-point grid spacing of $2\pi \times 0.015$ Å^{-1} is used. The dielectric function $\varepsilon(\omega) = \varepsilon_1(\omega) + \mathrm{i}\varepsilon_2(\omega)$ fully describes the optical properties of materials at all photon frequencies. The imaginary part $\varepsilon_2(\omega)$ of dielectric function can be derived from the electronic band structure by summing all allowed direct transitions from the occupied to the unoccupied states.

$$\varepsilon_2 = \frac{2e^2\pi}{\Omega\varepsilon_0} \sum_{k,v,c} |\langle \psi_k^c | u \cdot r | \psi_k^v \rangle|^2 \delta(E_k^c - E_k^v - E), \qquad (1)$$

where e is the electronic charge, u is the vector determining the polarization of the incident electric field, ω is the light frequency, and Ψ_k^c and Ψ_k^v are the conduction and valence band wave functions at k, respectively. The real part $\varepsilon_1(\omega)$ of dielectric function can be computed according to the Kramer–Kronig transformation

$$\varepsilon_1 = 1 + \frac{2}{\pi} p \int_0^\infty \frac{\omega' \varepsilon_2(\omega')}{\omega'^2 - \omega^2} \mathrm{d}\omega'. \qquad (2)$$

The other macroscopic optical constants, such as refractive index $n(\omega)$, extinction coefficient $k(\omega)$, absorption coefficient $a(\omega)$, reflection coefficient $R(\omega)$ and energy loss functions can be calculated once the complex dielectric function is obtained.[22,23]

3. Results and discussion

3.1. Structural properties

The pyrochlore-type $Bi_2Sn_2O_7$ shown in Fig. 1 has a cubic structure with space group Fd-$3m$, in which Bi atoms are located at the 16c site, Sn atoms at the 16d site, and O atoms at the 8a and 48f sites. The O (48f) atoms form octahedrons connecting each other with vertices, and Sn atoms are in the center of the octahedrons. The O (8a) and O (48f) atoms constitute the 8-coordinated dodecahedrons in which Bi atoms are just located in their centers. Moreover, the dodecahedrons connect with the neighboring dodecahedrons and octahedrons with edges. The optimized lattice parameters are listed in Table 1 and are in good agreement with the experimental data.[24] In the BiO_8 dodecahedrons, the optimized interatomic distance between Bi and O (8a) atoms is about 2.327 Å and obviously shorter than that between Bi and O (48f) atoms (2.621 Å). The bond length between Sn and O (48f) atoms is about 2.095 Å.

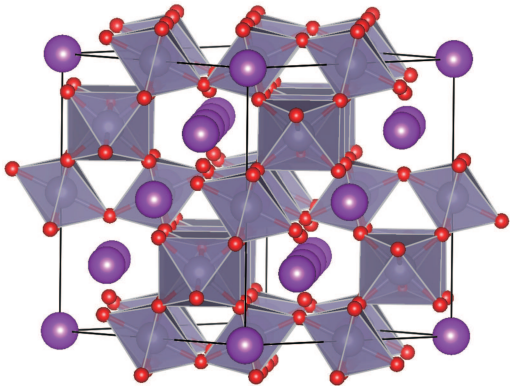


Fig. 1. (color online) Crystal structure of the pyrochlore-type γ-$Bi_2Sn_2O_7$. The octahedrons sharing vertices represent SnO_6 subunits, where Sn atoms are located in the center and O atoms at the vertices.

Table 1. Optimized structural parameters of γ-$Bi_2Sn_2O_7$. The experimental values[24] are given in the following parentheses for comparison.

Structure	Lattice constants/Å	Wyckoff positions				
		Atom	Site	x	y	z
γ-$Bi_2Sn_2O_7$ (Fd-$3m$)	a = 10.7489 (10.7225)	Bi	16c	0	0	0
		Sn	16d	1/2	1/2	1/2
		O	8a	1/8	1/8	1/8
		O	48f	0.4178 (0.4126)	1/8	1/8

3.2. Electronic and optical properties

The calculated electronic band structure of γ-$Bi_2Sn_2O_7$ is plotted in Fig. 2. The valence band maximum (VBM) is located at the X point and the conduction band minimum (CBM) is at the Γ point in the Brillouin zone and the Fermi level (E_F) is at the top of the valence band, which means that the pyrochlore-type $Bi_2Sn_2O_7$ is the p-type semiconductor with an indirect gap. The calculated band gap is about 2.72 eV and agrees well with the experimental data (2.78 eV)[12] and previously calculated value (2.74 eV).[15] The bands near E_F are relatively flat and possess a high concentration of carriers, which is beneficial for light absorption. The calculated values of the effective mass of carrier (m^*) are listed in Table 2 and helpful to understand the electrical properties of γ-$Bi_2Sn_2O_7$. The effective mass values in different directions are identical, indicating isotropic electric behavior of cubic γ-$Bi_2Sn_2O_7$. The effective mass of hole (m_h^*) is obviously heavier than that of electron (m_e^*) regardless of being at Γ or the X point, which shows that the electrons play a major role in determining the electrical conductivity for γ-$Bi_2Sn_2O_7$.

Figure 3 shows the total and partial density of states (DOS) of γ-$Bi_2Sn_2O_7$. The valence bands (VBs) centered at about −9.2 eV are mainly from the 6s states of Bi atoms and the 2s and 2p states of O (8a) atoms. The VBs approximately ranging from −7.4 eV to −5.3 eV are formed mainly due to the hybridization between the 5s states of Sn atoms and the 2p states of O (48f) atoms. In the energy region from about −5.2 eV to −1.6 eV, the total DOS is mainly from the Bi-6p, Sn-5p, O (8a)-2p, and O (48f)-2p states. The hybridization interaction between Sn-4d and O (48f)-2p states is also ob-

vious in a narrow energy region from −1.4 eV to −0.5 eV. The VBs in the energy region from −0.9 eV up to the E_F are mainly comprised of the Bi-6s, O (8a)-2p, and O (48f)-2p states, and essential to determining the electrical properties of γ-$Bi_2Sn_2O_7$. It can also be found from Fig. 3 that the conduction bands (CBs) close to the CBM are mainly created with the Bi-6p, Sn-5s, O (8a)-2p,and O (48f)-2p states.

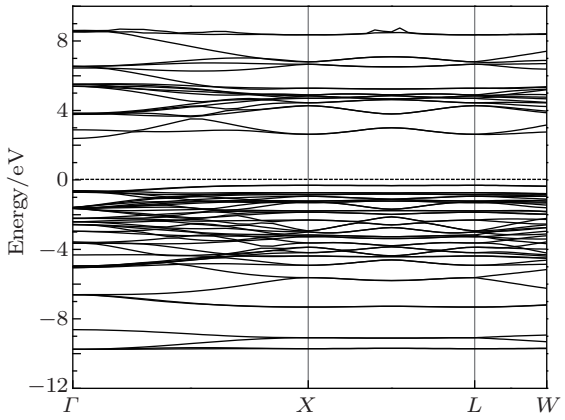


Fig. 2. Calculated electronic band structure of γ-$Bi_2Sn_2O_7$ along the selected high symmetry lines. The Fermi level is set to be zero for reference.

Table 2. Calculated effective mass tensors of electrons (m_e^*) in the conduction band and holes (m_h^*) in the valence band near the E_F at Γ (0, 0, 0) and X (0.5, 0, 0.5) points as marked in Fig. 1. All values are in units of free electron mass m_0.

	m_e^*	m_h^*
Γ	$\begin{pmatrix} 0.389 & 0 & 0 \\ 0 & 0.389 & 0 \\ 0 & 0 & 0.389 \end{pmatrix}$	$\begin{pmatrix} -1.758 & 0 & 0 \\ 0 & -1.758 & 0 \\ 0 & 0 & -1.758 \end{pmatrix}$
X	$\begin{pmatrix} 0.289 & 0 & 0 \\ 0 & 0.289 & 0 \\ 0 & 0 & 0.289 \end{pmatrix}$	$\begin{pmatrix} -2.125 & 0 & 0 \\ 0 & -2.125 & 0 \\ 0 & 0 & -2.125 \end{pmatrix}$

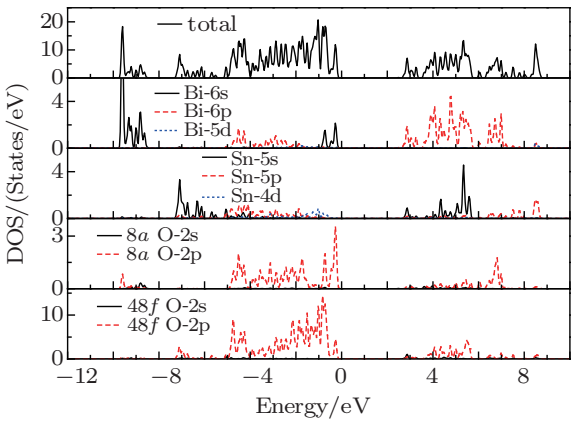


Fig. 3. (color online) Calculated total and partial DOS of γ-$Bi_2Sn_2O_7$.

Figure 4 shows the calculated real part $\varepsilon_1(\omega)$ and imaginary part $\varepsilon_2(\omega)$ of the complex dielectric function for cubic γ-$Bi_2Sn_2O_7$, each as a function of photon energy up to 35 eV. The static dielectric function is found to be 5.5 at 0 eV. The origin of the observed peak in the imaginary part $\varepsilon_2(\omega)$ of the dielectric function can be explained with the help of the calculated DOS shown in Fig. 3, since $\varepsilon_2(\omega)$ is correlated to the crystal absorption spectrum. The first two stronger absorption peaks centered at about 3.7 eV and 5.6 eV in $\varepsilon_2(\omega)$ are probably ascribed to the transitions from the occupied states of the valence band group to the unoccupied electronic states at the bottom of the conduction band (CB).

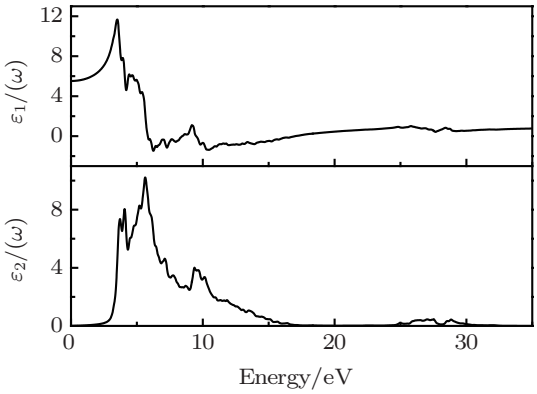


Fig. 4. Calculated dependences of real part $\varepsilon_1(\omega)$ and imaginary part $\varepsilon_2(\omega)$ of the dielectric function of γ-$Bi_2Sn_2O_7$ alloys on photon energy.

Based on the obtained dielectric function, the refractive index $n(\omega)$, extinction coefficient $k(\omega)$, absorption coefficients $\alpha(\omega)$, reflectivity $R(\omega)$, and electron energy-loss function $L(\omega)$ are further calculated to check the optical properties of γ-$Bi_2Sn_2O_7$ (see Fig. 5). The static refractive index $n(0)$ is about 2.4, which is closely related to the real part $\varepsilon_1(\omega)$ of the dielectric function. $n(\omega)$ reaches its maximum value of 3.6 at 3.5 eV and then drops drastically with the increase of photon energy. The calculated $k(\omega)$ is below 0.1 in a photon energy range from 0 to about 3 eV, meaning that γ-$Bi_2Sn_2O_7$ will have a response to the light with wavelength less than 414 nm. Then $k(\omega)$ increases rapidly with increasing photon energy, forms the first peak in the near UV region at approximately 4.1 eV, and reaches the maximum value of about 2.1 at 5.8 eV. Our calculated results indicate that cubic γ-$Bi_2Sn_2O_7$ has strong extinction effects on the part of violet light in the visible light region, the part near the UV region, and most of the part of the far UV region. The calculated absorption intensity of $\alpha(\omega)$ in the infrared and most visible region is nearly zero and starts to go up rapidly at about 2.5 eV. There is a broad absorption peak ranging from about 3.7 eV to 25 eV. Especially, the first two strong peaks at about 6.2 eV and 9.8 eV are related to the transitions of Sn-5s and Bi-6s orbitals. The majority of the absorption spectrum of cubic $Bi_2Sn_2O_7$ is in the UV region, which suggests that cubic $Bi_2Sn_2O_7$ may have special applications in certain optical components. The calculated $R(\omega)$ shows that the average reflectivity is about 30%, which is an acceptable value for light absorbing material. Two small peaks at about 27.6 eV and 29.1 eV except the strong main peak at about 16.9 eV in the calculated $L(\omega)$ presented in Fig. 5 can be found, which corresponds to the energy of the plasma edge and shows the characteristics of plasma oscillation in γ-$Bi_2Sn_2O_7$.

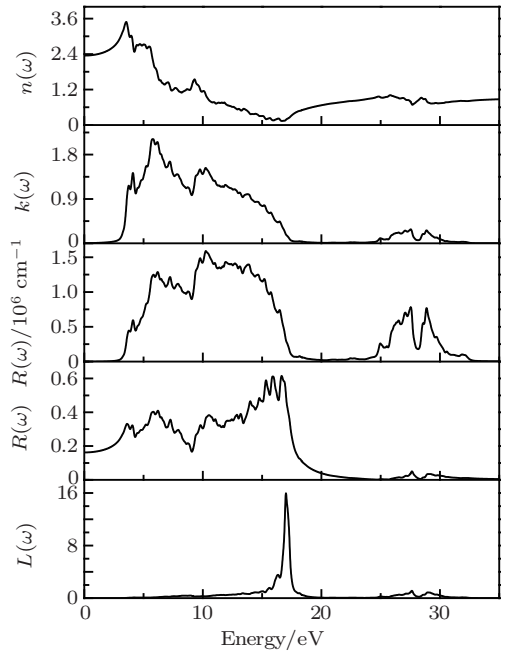


Fig. 5. Calculated refractive index $n(\omega)$, extinction coefficient $k(\omega)$, absorption coefficient $\alpha(\omega)$, reflectivity $R(\omega)$, and electron energy-loss function $L(\omega)$ of γ-$Bi_2Sn_2O_7$, each as a function of photon energy.

3.3. Mechanical properties

The calculated elastic constants C_{ij} of γ-$Bi_2Sn_2O_7$ are listed in Table 3.

Table 3. Calculated values of elastic constant C_{ij}, bulk modulus B, shear modulus G, Young's modulus E, and Poisson's ratio υ of γ-$Bi_2Sn_2O_7$.

C_{11}	C_{12}	C_{44}	B	G	E	υ
259.2	107.7	72.5	158.2	73.8	191.6	0.3

The bulk modulus B and shear modulus G are obtained by Voigt–Reuss–Hill approximation.[25] Young's modulus E and Poisson's ratio υ can be further calculated according to their relationships with B and G. The corresponding mechanical stability criterion for cubic crystal is that B, C_{11}–C_{12}, and C_{44} are positive.[26] It can be found from Table 3 that γ-$Bi_2Sn_2O_7$ satisfies the condition for elastic stability. The calculated B and G of γ-$Bi_2Sn_2O_7$ are 158.2 GPa and 73.8 GPa respectively, and the value of B/G is about 2.14, obviously indicating that cubic $Bi_2Sn_2O_7$ belongs to a kind of ductile material, since the material is ductile if its B/G value is higher than 1.75 according to Pugh's criteria of brittleness and ductility.[27] Furthermore, the calculated Poisson's ratio is about 0.3 and also shows the ductile characteristic of cubic $Bi_2Sn_2O_7$. According to Zener's definition,[28] the anisotropy of material can be described by the parameter $A = G_1/G_2$, where $G_1 = C_{44}$, $G_2 = (C_{11}–C_{12})/2$. Generally, the isotropic material has a value of $A = 1$. For γ-$Bi_2Sn_2O_7$, the calculated A is about 0.96, showing high isotropy. In addition, according to the relationship between Young's modulus and elastic compliance constants,[29] the elastic anisotropy of γ-$Bi_2Sn_2O_7$ can be directly checked by the directional dependence of Young's modulus. The calculated results depicted in Fig. 6 show that the directional dependence of Young's modulus almost exhibits a spherical shape, which indicates that γ-$Bi_2Sn_2O_7$ is highly isotropic.

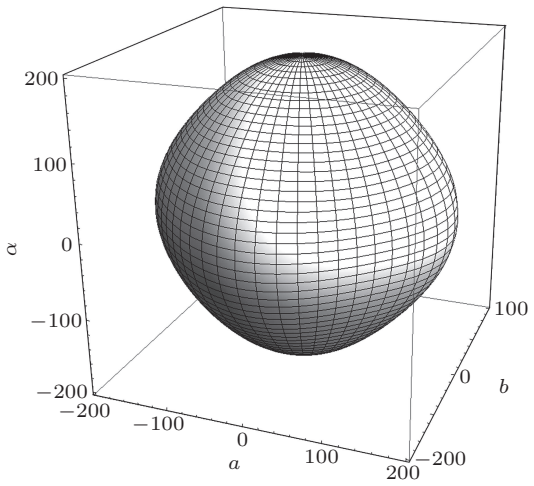


Fig. 6. Directional dependence of Young's modulus of cubic γ-$Bi_2Sn_2O_7$.

4. Conclusions

The electronic, optical, and mechanical properties of γ-$Bi_2Sn_2O_7$ are investigated by using the first-principles DFT calculations. Our results show that γ-$Bi_2Sn_2O_7$ is the p-type semiconductor with an indirect band gap. The calculated band gap is about 2.72 eV and in excellent agreement with the experimental result. The hybridization interaction between Bi-6s and O-2p states in the valence bands close to the Fermi level is expected to play an essential role in determining the electrical behavior of γ-$Bi_2Sn_2O_7$. The dielectric function and macroscopic optical constants including refractive index, extinction coefficient, absorption coefficients, reflectivity, and electron energy-loss function are also calculated to check the optical properties of γ-$Bi_2Sn_2O_7$. Especially, the average reflectivity is about 30%, which indicates that γ-$Bi_2Sn_2O_7$ is a good light absorbing material used for optical semiconductor devices and photocatalysts. Moreover, γ-$Bi_2Sn_2O_7$ is mechanically stable and ductile according to the calculated elastic constants, bulk modulus, Young's modulus, and Poisson's ratio. The further calculations of the directional dependence of Young's modulus show that γ-$Bi_2Sn_2O_7$ is highly isotropic.

References

[1] Abe R, Higashi M, Zou Z, Sayama K and Abe Y 2004 *Chem. Lett.* **33** 954
[2] Park S, Song H, Choi H and Moon J 2004 *Solid State Ionics* **175** 625
[3] Bramwell S T and Gingras M J P 2001 *Science* **294** 1495
[4] Hanawa M, Muraoka Y, Tayama T, Sakakibara T, Yamamura J and Hiroi Z 2001 *Phys. Rev. Lett.* **87** 187001
[5] Roth R S 1956 *J. Res. Nat. Bur. Stand.* **56** 17
[6] Brisse F and Knop O 1968 *Can. J. Chem.* **46** 859
[7] Subramaniam M A, Aravamudan G and Subba Rao G V 1983 *Prog. Solid State Chem.* **15** 55

[8] Kahlenberg V and Zeiske T 1997 *Z. Kristallogr.* **212** 297
[9] Gao F, Chen X Y, Yin K B, Dong S, Ren Z F, Yuan F, Yu T, Zou Z G and Liu J M 2007 *Adv. Mater.* **19** 2889
[10] Tang J W, Zou Z G and Ye J H 2004 *Catal. Lett.* **92** 53
[11] Yu J and Kudo A 2006 *Adv. Funct. Mater.* **16** 2163
[12] Wu J, Huang F, Lü X, Chen P, Wan D and Xu F 2011 *J. Mater. Chem.* **21** 3872
[13] Tian Q, Zhuang J, Wang J, Xie L and Liu P 2012 *Appl. Catal. A: Gen.* **425–426** 74
[14] Xu W, Fang J, Zhu X, Fang Z and Chen C 2015 *Mater. Res. Bull.* **72** 229
[15] Walsh A and Watson G W 2007 *Chem. Mater.* **19** 5158
[16] Fan W, Hu J, Huang J, Wu X, Lin S, Huang C and Qiu X 2015 *Appl. Surf. Sci.* **357** 2364
[17] Kresse G and Joubert D 1999 *Phys. Rev. B* **59** 1758
[18] Kresse G and Hafner J 1994 *Phys. Rev. B* **49** 14251
[19] Kresse G and Furthmüller J 1996 *Comput. Mater. Sci.* **6** 15
[20] Perdew J P, Burke K and Ernzerhof M 1996 *Phys. Rev. Lett.* **77** 3865
[21] Monkhorst H J and Pack J D 1976 *Phys. Rev. B* **13** 5188
[22] Adolph B, Furthmüller J and Bechstedt F 2001 *Phys. Rev. B* **63** 125108
[23] Gajdoš M, Hummer K, Kresse G, Furthmüller J and Bechstedt F 2006 *Phys. Rev. B* **73** 045112
[24] Kahlenberg V and Zeiske T Z 1997 *Z. Kristallogr.* **212** 297
[25] Hill R 1952 *Proc. Phys. Soc. London* **65** 349
[26] Wallace D C 1972 *Thermodynamics of Crystals* (New York: Wiley)
[27] Pugh S F 1954 *Philos. Mag.* **45** 823
[28] Zener C 1948 *Elasticity and Anelasticity of Metals* (Chicago: University of Chicago Press)
[29] Ranganathan S I and Ostoja-Starzewski M 2008 *Phys. Rev. Lett.* **101** 055504